Dyes and Pigments 115 (2015) 166–171

Contents lists available at ScienceDirect

Dyes and Pigments

journal homepage: www.elsevier.com/locate/dyepig

Linear thiophene-containing π-conjugated aldehydes with aggregation-induced emission for building solid red luminophors

Kunpeng Guo [a], [*], Zhixiang Gao [b], Jun Cheng [a], Yang Shao [c], Xiaoqing Lu [c], [*], Hua Wang [a]

[a] Ministry of Education Key Laboratory of Interface Science and Engineering in Advanced Materials, Research Center of Advanced Materials Science and Technology, Taiyuan University of Technology, Taiyuan 030024, PR China
[b] School of Physics and Electronic Science, Shanxi Datong University, Datong 037009, PR China
[c] College of Science, China University of Petroleum, Qingdao 266580, PR China

ARTICLE INFO

Article history:
Received 18 September 2014
Received in revised form
11 December 2014
Accepted 16 December 2014
Available online 25 December 2014

Keywords:
Linear π-conjugated aldehyde
Aggregation-induced emission
Amorphous aggregates
Thiophene
1,3-Indandione
Solid red emitter

ABSTRACT

Two linear thiophene-containing π-conjugated aldehydes 4-(thiophen-2-yl)benzaldehyde and 2,5-bis[4-(formyl)phenyl]thiophene exhibiting aggregation-induced emission (AIE) were demonstrated. The photophysical properties of the two aldehydes in solution and THF/H_2O mixtures were studied, and aggregates formed with different water fractions were studied by scanning electron microscopy. Results indicated that amorphous nanoscale aggregates exhibit distinct AIE behavior when assembled in solutions with appropriate water contents. Condensation of 1,3-indandione with 4-(thiophen-2-yl)benzaldehyde generated a new luminophor 2-[4-(thiophen-2-yl)benzylidene]-2H-indene-1,3-dione; this product presents as a solid powder that emits intensely red photoluminescence at 620 nm with a quantum yield of 12.8%.

1. Introduction

The design and synthesis of π-conjugated luminophors has generated considerable research and commercial interest because of the applicability of these materials in various optoelectronic and biological devices, such as organic lighting-emitting diodes (OLEDs), upconverted lasers, chemosensors, and bioprobes [1–4]. Although a number of π-conjugated materials are known to show highly efficient fluorescence in dilute solutions, most of them tend to show decreased or quenched fluorescence in the aggregated or solid state [5]. Aggregation-caused quenching (ACQ) has greatly limited the practical applications of π-conjugated materials because most of these materials must be used in the aggregated or solid state. The present study seeks to address the challenge of developing π-conjugated materials.

In 2001, aggregation-induced emission (AIE) was reported by Tang's group to be a promising method to eliminate ACQ. Induced nonluminescent molecules with propeller-like conformations have been shown to exhibit efficient emission because of aggregate formation [6]. The molecular structures and optoelectronic properties of various materials can be easily analyzed through determination of their building blocks. Following the pioneering work of Tang's group, various aggregated and solid-state emissive luminophors, particularly AIE materials, have been prepared through rational coupling, such as with propeller-like AIE building blocks [7–9]. To satisfy the demand for optoelectronic active materials, π-conjugated materials without propeller-like conformations exhibiting AIE characteristics have also been studied extensively [10–13]. Linear π-conjugated materials are well known backbones for covalent construction of multifunctional small molecules and polymers [14–18]. Materials that possess prominent AIE characteristics and feature cost-efficient preparations present great potential significance; however, these materials are rarely reported in the literature.

Red to near-infrared (NIR) fluorescent dye emissions in the aggregated or solid state are of significant importance in fundamental investigations and practical applications, such as in red OLED and bioimaging, owing to little interferences from optical absorption and light scattering [19–22]. However, most of the AIE materials prepared thus far dominantly emit blue or green light, and production of solid emitters with longer wavelengths is limited by complicated synthesis steps [23]. In the present study, we

---

[*] Corresponding authors.
E-mail address: guokunpeng@tyut.edu.cn (K. Guo).

http://dx.doi.org/10.1016/j.dyepig.2014.12.017

develop a solid red emitter based on a linear π-conjugated backbone with fewer synthetic difficulties. We address the problems identified in the preceding paragraph by studying two linear thiophene-containing π-conjugated aldehydes 4-(thiophen-2-yl) benzaldehyde (TBA) and 2,5-bis[4-(formyl)phenyl)]thiophene (biFPT), the structures of which are depicted in Fig. 1. Structurally, thiophene and its aldehyde derivatives are highly reactive organic building blocks that provide several advantages for synthesizing chemical materials such as hole transporters, organic luminophors, light-harvesting dyes, metal-organic frameworks, and sensors [24–28]. To the best of our knowledge, this work is the first to report linear thiophene-containing aldehydes with prominent AIE characteristics. A novel solid red luminophor, 2-[4-(thiophen-2-yl) benzylidene]-2H-indene-1,3-dione (TBID), is generated via one-step Knoevenagel condensation between TBA and 1,3-indandione; this luminopher exhibits higher quantum yield (Φ_F) in its solid state than in solution.

2. Experimental

2.1. Materials and apparatus

1, 3-Indandione was purchased from J&K Chemical. Reactions were monitored by TLC silica plate (60F-254). Column chromatography was performed on silica gel (100–200 mesh). NMR spectra measurements were carried out at Bruker 600 MHz for ^{1}H NMR and 100 MHz for ^{13}C NMR, using Chloroform-*d* as solvent. Chemical shifts were reported in parts per million (ppm) relative to internal TMS (0 ppm). Splitting patterns were described as singlet (s), doublet (d), triplet (t), quartet (q), or multiplet (m). Mass spectra measured on Microflex MALDI-TOF MS. Elemental analysis was run on a Vario EL III Elemental Analyzer. Melting point was measured on X4 melting point apparatus. UV–Vis spectra were recorded in a HITIACH U-3900 spectrometer. Photoluminescent (PL) spectra were recorded in a HORIBA FluoroMax-4 spectrometer. The absolute florescence quantum yields of solutions (10 μM) and solid powders were measured on HORIBA FluoroMax-4 (excited at 365 nm) by using a calibrated integrating sphere. The quartz cuvettes used were of 1 cm path length. The scanning electron microscopy (SEM) studies were performed using a JEOL JEM-6700F scanning electron microscope. One drop of the solution was placed on a silicon slice, which was then dried in air.

X-ray single-crystal diffractions of biFPT was performed on Bruker SMART APEX II diffractometer with Mo Ka radiation (λ = 0.71000 Å). The structure was solved with direct method (SHELX-97) and refined with full-matrix least-squares technique. All non-hydrogen atoms were refined anistropically and hydrogen atoms were geometrically placed. Relevant crystal collection data, refinement data for the crystal structures and the cif files of biFPT can be found in the ESI.

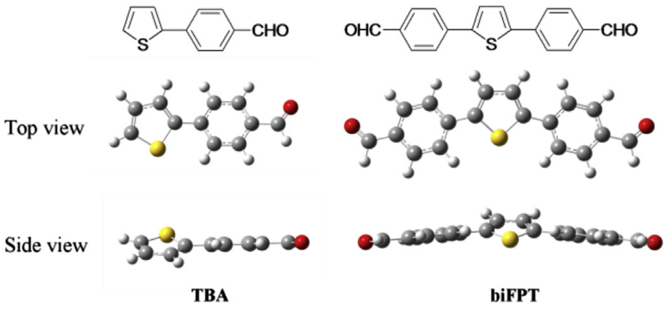

Fig. 1. Optimized molecular geometry of TBA and biFPT based on the B3LYP/6-31G* level.

2.2. Synthesis

2.2.1. Synthesis of 2-(4-(thiophen-2-yl)benzylidene)-2H-indene-1,3-dione (TBID)

A C_2H_5OH (10 mL) solution of compound TBA (150.4 mg, 0.8 mmol), 1, 3-Indandione (52.5 mg, 0.36 mmol) and two drops of acetic acid and triethylamine were charged sequentially into a three-necked flask and heated to reflux till no starting material 1, 3-indandione was detected by the TLC plate. After cooling to room temperature, solvents were removed by rotary evaporation, and the residue was purified by silica gel column chromatography with petroleum ether: EtOAc (4: 1, v:v) as eluent to afford TBID as yellow powder (95.6 mg, yield 70.6%). ^{1}H-NMR (400 MHz, $CDCl_3$, ppm): δ = 8.51 (d, 2H, *J* = 8.4 Hz); 8.02 (m, 2H); 7.89 (s, 1H); 7.82 (d, 2H, *J* = 8.4 Hz), 7.76 (d, 2H, *J* = 8.4 Hz), 7.50 (dd, 1H), 7.39 (dd, 1H), 7.14 (t, 1H, *J* = 8.4 Hz),. ^{13}C-NMR (100 MHz, $CDCl_3$, ppm): δ = 193.16; 191.96; 148.81; 148.17; 145.50; 143.04; 141.78; 138.15; 137.96; 135.12; 131.70; 131.36; 129.72; 128.65; 127.85; 126.14. MALDI-TOF: m/z $[M]^+$ cacld. $C_{20}H_{12}O_2S$, 316.0558; found: 316.0555. ELEM. ANAL: cacld. $C_{20}H_{12}O_2S$, C, 75.93%; H, 3.82%; O, 10.11%; S, 10.14%; found: C, 75. 76%; H, 3.81%; O, 10.26%, S, 10.17%.

3. Results and discussion

3.1. Molecular geometry of TBA and biFPT

TBA and biFPT were synthesized via one-step Suzuki coupling [29,26]. To understand the configurations of these two aldehydes better, molecular geometries were first evaluated at the B3LYP/6-31G* level. The optimized molecular geometries of TBA and biFPT are shown in Fig. 1. The dihedral angles of TBA and biFPT between the marginal phenyl unit and the central thienyl ring are 24.7° and 25.6°, respectively. Fig. 2 and Table S1 show the summarized crystallographic data of the growth process of single crystals of biFPT by slow evaporation of its hexane solution. Fig. 2 reveals that the torsion angles between T1 and the adjacent phenyl groups P1 and P2 are 17.8° and 19.6°, respectively. These results clearly indicate that the two aldehydes adopt certain linear and planar conformations.

3.2. Photophysical properties of TBA and biFPT

Both aldehydes are soluble in common solvents such as acetone, dichloromethane, and tetrahydrofuran (THF) but insoluble in water. The absorption and emission spectra of TBA and biFPT in dilute THF (10 μM) at room temperature are shown in Fig. 3. TBA and biFPT present relatively strong absorption in the 300–400 nm region, which corresponds to π-π* transitions. The absorption maximum (λ_{max}) is observed at 323 nm (molar extinction coefficient $\varepsilon = 2.3 \times 10^4$ M^{-1} cm^{-1}) for TBA and red-shifts to 373 nm ($\varepsilon = 2.7 \times 10^4$ M^{-1} cm^{-1}) for biFPT; such results reveal the extended conjugation of biFPT compared with that of TBA. The maximum emission wavelengths (λ_{em}) of TBA and biFPT are located at 430 and 435 nm, respectively. biFPT also shows evidently higher PL intensity than TBA. The Φ_F value of bFiPT (6.78%) is higher than that of TBA

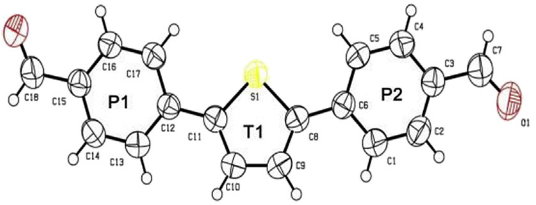

Fig. 2. ORTEP diagram of biFPT.